C. C. Raible · R. Blender

Northern Hemisphere midlatitude cyclone variability in GCM simulations with different ocean representations

Abstract The impact of different ocean models or sea surface temperature (SST) and sea-ice concentrations on cyclone tracks in the Northern Hemisphere midlatitudes is determined within a hierarchy of model simulations. A reference simulation with the coupled atmosphere ocean circulation model ECHAM/HOPE is compared with simulations using ECHAM and three simplified ocean and sea-ice representations: (1) a variable depth mixed layer (ML) ocean, (2) forcing by varying SST and sea-ice, and (3) with climatological SST and sea-ice; the latter two are from the coupled ECHAM/HOPE integration. The reference simulation reproduces the observed cyclone tracks. The cyclones are tracked automatically by a standard routine and the variability of individual cyclone trajectories within the storm tracks is determined by a cluster approach. In the forced simulation with varying SST, the geographical distribution and the statistics of the cyclones are not altered compared to the coupled reference simulation. In the ML- and the climatological simulation, deviations of the mean cyclone distribution are found which occur mainly in the North Pacific, and can partially be traced back to missing El Niño/Southern Oscillation (ENSO) variability. The climatological experiment is superior to the ML-experiment. The variability of the individual cyclone trajectories, as determined by the cluster analysis, reveals the same types and frequencies of propagation directions for all four representations of the lower boundary. The largest discrepancies for the cluster occupations are found for the climatological and the ML-simulation.

C. C. Raible (✉)
Climate and Environmental Physics, Physics Institute,
University of Bern, Sidlerstrasse 5,
3012 Bern, Switzerland
E-mail: raible@climate.unibe.ch

R. Blender
Meteorologisches Institut, Universität Hamburg,
Bundesstrasse 55, 20146 Hamburg, Germany

1 Introduction

Synoptic cyclones are the dominant cause of midlatitude high-frequency variability and a key element for continental climate conditions. Most of the Northern Hemispheric cyclones originate in the western ocean basins and move northeastward across the North Atlantic or the North Pacific basins. Since the interannual variability of these cyclones is considerable, it is rather difficult to determine means and significant trends, for example anthropogenic changes of the positions and intensities. The development of cyclones as well as their paths are influenced by oceanic boundary conditions, mainly the sea surface temperature (SST). On the other hand, the atmosphere acts on the ocean, predominantly due to the wind stress and freshwater flux. Thus, the simulation of cyclones requires coupled dynamical atmosphere-ocean general circulation models (AOGCMs).

However, many simulations are performed with simpler ocean representations such as mixed layer or slab ocean models. Such approximations, which are frequently based on computational demands, are plausible since the ocean evolves slower than the atmosphere. Alternatives are independent SSTs, given either from observations (for example in the Atmospheric Modelling Intercomparison Project, AMIP), simulated SST time series or climatologies. A comparison of the winter cyclone event statistics in re-analyses (ERA15 by the European Centre for Medium-Range Weather Forecasts, ECMWF, and of the National Center for Environmental Predictions, NCEP) with 13 AMIP simulations has been performed by Lambert et al. (2002). The large-scale features are reasonably well simulated by the majority of the models with deficiencies at the ends of the storm tracks and in mountain lee cyclogenesis (note that there are differences between both re-analyses).

In general, we can expect that the decoupling of climate system components changes the dynamics, the

mean state and, in most cases, reduces the variability. This problem was studied in a conceptual framework by Roebber et al. (1997) with low-order models for the atmosphere and the ocean. These authors find that the atmospheric variability alters substantially compared to the coupled case if the atmosphere is forced with a climatological SST.

This leads us to question, whether and to what extent a reduced or simplified ocean model is able to yield the cyclone characteristics and their variability shown in complex AOGCMs. As a simple measure for the cyclonic activity, storm tracks, defined as standard deviations of the band-pass filtered (2.5 to 6 days) 500 hPa geopotential height, are widely used (Blackmon 1976). These Eulerian patterns, however, merge all kinds of variability, including waves and high pressure cells. On the other hand cyclone tracks are determined either manually or automatically and use surface pressure, vorticity, or geopotential height to define and track low pressure systems (Murray and Simmonds 1991; König et al. 1993; Hodges 1994; Haak and Ulbrich 1996; Blender et al. 1997; Sinclair 1997).

The aim of this work is to determine the influence of simplified ocean representations on the Northern Hemispheric midlatitude cyclone tracks. We compare the fully coupled AOGCM ECHAM/HOPE (Legutke and Voss 1999) with ECHAM coupled to a mixed layer (ML) ocean (Karaca and Müller 1991), ECHAM forced by a varying lower boundary, and ECHAM forced by a climatological lower boundary; the two latter lower boundaries (SST, sea-ice cover, sea-ice thickness, and sea-ice albedo) are derived from the ECHAM/HOPE integration. To obtain reliable statistics, the simulation time is 100 years. The cyclones are tracked automatically by a standard routine and the cyclone variability is determined by a cluster approach (Blender et al. 1997).

The outline of this study is as follows: The three models ECHAM, HOPE and ML are described in Sect. 2. The experimental design which defines the coupling of the ECHAM in the four simulations is in Sect. 3. The measures of cyclone intensity and variability are introduced in Sect. 4. Section 5 validates the ECHAM/HOPE simulation and presents the results for the storm tracks, the cyclone intensities, and the variability of the relative cyclone trajectories for all experiments. Finally, the results are summarised and discussed in Sect. 6.

2 Models

The atmosphere and ocean models are state-of-the-art and widely used in climate simulations. In all experiments, the atmosphere is simulated by the general circulation model ECHAM, which can be coupled to the ocean circulation model HOPE or to a simple mixed layer ocean model. Some details of these models are:

Atmosphere-GCM. The atmosphere is simulated by the fourth version of the *E*uropean *C*entre model of *Ham*burg (ECHAM)

climate model (Roeckner et al. 1996). This spectral model is used with triangular truncation at wave number 30 (T30), corresponding to a longitude-latitude grid of approximately 3.75° × 3.75° and with 19 hybrid sigma-pressure levels in the vertical up to 10 hPa. The T30-resolution is chosen as a balance between computational costs and realistically simulated climate statistics. The storm tracks are compared with ERA15 (ECMWF) re-analyses and show satisfactory agreement (Stendel and Roeckner 1998).

Ocean-GCM. The dynamic ocean circulation model is the *H*amburg *o*cean model in *p*rimitive *e*quations (HOPE) simplified by the Boussinesq approximation and formulated on a Gaussian T42 Arakawa-E grid (Wolff et al. 1997). The horizontal resolution is approximately 2.8° × 2.8°, increasing to 0.5° meridionally in the tropics. In the vertical the model consists of 20 irregularly distributed levels with 10 levels in the first 300 m.

Mixed layer (ML) Model. The classical ML-model of (Karaca and Müller 1991) is extended by a dynamical mixed-layer depth (Dommenget 2000). This model includes local atmospheric forcing and the exchange with the underlying layer. The variability of the SST is damped by the sub-layer exchange in the case of storms. The model is adjusted to the climatology of the coupled HOPE experiment. Clearly, the ML-model is not able to simulate the thermohaline circulation or ENSO-like variability.

3 Experimental design

The design of the experiments requires a balance between spatial resolution and time range. Since the interannual variability of the cyclones is high, the detection of reliable spatial fields of mean cyclone frequencies needs decades. For the analysis of changes induced by different model environments, rather long integrations of the order of 100 years are suitable.

On the other hand, a spatial resolution of T30 (3.75° × 3.75° degrees) is considered as sufficient for the representation of synoptic cyclones (Stendel and Roeckner 1998, deviations from ERA15 are below 10%). Any improvement of the resolution leads to an increase of the number of cyclones. This is not only due to the inclusion of smaller and weaker cyclones, but also due to the inclusion of more orographically induced cyclones, because the orographic heights are increased at the same time. In particular in the North Atlantic a large number of cyclones is created by the Greenland massive. These cyclones, which contribute substantially to the NAO variability (Sickmöller et al. 2000), are not simulated with T30 resolution.

Four experiments are carried out which represent standard approaches and simplifications of the ocean and sea-ice components in climate studies. A coupled ECHAM/HOPE experiment is the reference for the simpler models. For the comparison of the four experiments it is necessary to perform consistent simulations with no long-term mean bias between the coupled reference experiment and the three simplified experiments. The experiments are in detail (Fig. 1):

Coupled HOPE-Experiment. ECHAM and HOPE are coupled through OASIS (Ocean Atmosphere Sea-Ice Soil) of Terray et al. (1998) and annual mean flux correction schemes for heat and fresh water; the atmospheric component, ECHAM, is modified compared to the standard version in order to account for sub-grid scale partial ice cover. A 600 year simulation for present-day climate conditions is carried out (Legutke and Voss 1999; Raible et al. 2001) and the 100 year period from model year 130 to 229 is used as a reference in the remainder of this study.

Coupled ML-Experiment. The atmospheric model ECHAM is coupled with the dynamical ML-model and integrated for 100 years. Besides the complex atmospheric dynamics the simulation contains reduced ocean dynamics, that is local thermal
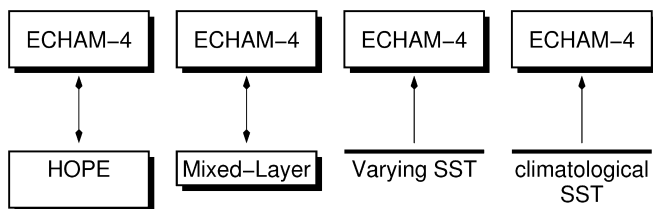
Fig. 1 Experimental design for the four experiments with different ocean presentations; the coupled ECHAM/HOPE experiment is the reference

forcing and memory. The ML-model is forced by the climatological conditions during the reference period of the coupled HOPE-experiment. However, the climate mean in this experiment deviates slightly from the forcing field.

Experiment with varying SST. ECHAM is forced by the varying SST, sea-ice cover, sea-ice thickness, and sea-ice albedo obtained by the coupled HOPE-experiment during the reference period. The 99 year simulation contains all physical processes of the atmosphere and the ocean but no atmospheric feedback to the ocean. This simulation incorporates all kinds of interannual variability, in particular ENSO. It delivers a test-bed for the impact of the interannual ocean variability.

Climatological Experiment. An annual cycle of the SST, sea-ice cover, sea-ice thickness, and sea-ice albedo is obtained by monthly means of the coupled HOPE-experiment. This boundary condition is used as a forcing in a 100 year simulation of ECHAM. Clearly, this experiment shows only internal atmospheric variability.

4 Cyclone variability

A simple measure of the cyclonic activity is the variability of a mid-tropospheric geopotential height field. Regions of enhanced variability are denoted as storm tracks. These include anomalies which cannot be attributed to cyclones, for example high-pressure cells and waves. The detection of individual cyclones requires an appropriate definition of the low-pressure systems and a procedure to identify systems in fields at subsequent time steps to reconstruct the trajectories. The temporal mean of these trajectories is denoted here as a cyclone track (as opposed to a storm track). Since the outcome of this Lagrangian approach is sensitive to the particular scheme used, the uniquely defined Eulerian storm track is preferred in many analyses. In the paragraphs that follow, the Eulerian storm track, the Lagrangian cyclone track, and a cluster analysis to determine the variability of the cyclone trajectories within a cyclone track are described.

4.1 Storm track

The storm track is defined here as a region with enhanced standard deviation of the band-pass filtered (2.5 to 6 days) 500 hPa geopotential height (Blackmon 1976; Wallace et al. 1988; Lau 1988). Due to the time filter, the storm track is restricted to the characteristic time scales of synoptic cyclones. Whereas the Southern Hemisphere shows a storm track with approximate zonal symmetry, the Northern Hemisphere shows an intense storm track in the North Atlantic and a weaker, more elongated storm track in the North Pacific.

4.2 Cyclone track

Automated cyclone tracking has been applied by Ueno (1993), König et al. (1993), and Sinclair (1994) who use a nearest-neighbour search method. A prediction and matching approach has been used by Murray and Simmonds (1991). A three-dimensional variational method has been developed by Hodges (1994). Most studies define lows as minima in the pressure or geopotential height; König et al. (1993) applied a combination of these minima and maxima in the vorticity. In the present study, the cyclone tracking algorithm of Blender et al. (1997) is applied. Lows are identified as minima of the 1000 hPa geopotential height (z1000) within a neighbourhood of eight grid points. Based on the work of Blender and Schubert (2000) we can estimate that at least 80% of the cyclones found here in 12 h time resolution are identical to those cyclones that would be found in a 2 h time resolution of the same data set (which can be considered to be exact). A mean gradient of at least 20 gpm/1000 km in a 1000 km neighbourhood is required to neglect weak minima. Regions with an altitude higher than 1000 m are excluded. The gradient is chosen as the intensity measure instead of the central pressure because the central pressure changes with the regional climate mean. The lows are connected to cyclone trajectories by a nearest-neighbour search in the preceding z1000-field within a distance of 1000 km. Furthermore, we require a minimum lifetime of three days and that a minimum gradient of 30 gpm/1000 km is exceeded at least once during the life cycle. The threshold for the mean z1000-gradient is low enough to detect cyclones in the initial phase and keep them during the weaker decay phase of their life cycle. Although errors cannot be avoided in automatic schemes, these methods are preferable if, as in this study, differences between data sets have to be determined, because these are only accessible with a fixed search method.

To determine the cyclone track intensity, the mean gradient of the geopotential height is averaged at every grid point. The occurrences are counted at each time step, even if the cyclone remains at the same position. These maps are extensions of the usual number densities which do not discriminate between weak and intense cyclones. The intensity maps are normalised by the total number of observation times (data fields) and the areas associated with the grid points. The result is given in units of gpm/1000^3 km^3 (geopotential height gradient in gpm/1000 km and area in 1000^2 km^2 which is roughly a 5°-latitude circle) and describes the mean gradient of

cyclones found at any arbitrary time within this area. In the figures, the values are multiplied by 100. For example, the contour value of 1000 gpm/1000^3 km^3 could be the result of an occupation of this area (1000^2 km^2) with cyclones of intensity 100 gpm/1000 km in 10% of the integration time.

4.3 Cyclone path variability

To determine the internal variability of cyclone trajectories within the cyclone tracks, a cluster analysis has been proposed by Blender et al. (1997). The cyclone trajectories are decomposed into three characteristic propagation patterns in the North Atlantic and the North Pacific (Sickmöller et al. 2000). These patterns are well reproduced by GCMs and climate change experiments are analyzed within this framework (Schubert et al. 1998).

The cluster analysis is applied to the first three days of all trajectories; the remaining parts are disregarded. A period of three days is sufficient to obtain a distinct separation of the trajectories. On the other hand the number of available cyclones is still sufficient (note that an increase of the minimum lifetime by one day reduces the number of cyclones by approximately one half). The cluster analysis is performed with the k-means algorithm (Hartigan and Wong 1979) which requires a specification of the number of clusters. A number of three cluster centroids appears to be meteorologically meaningful. The three cluster centroids correspond to three propagation types: northeastward (NE), zonal (ZO), and nearly stationary cyclones (ST). The number of the ST cyclones is highly sensitive to the resolution of the data since these cyclones are typically weak and small. The intensities and the mean square displacements of the cyclones in the three clusters show distinct characteristics (Blender et al. 1997).

5 Results

In a first step, the reference simulation is validated with NCEP re-analyses. We compare the time mean storm track variability, the cyclone intensities, and, additionally, the relation to teleconnection patterns given by NAO (North Atlantic Oscillation) and El Niño anomalies. The latter is necessary, since a considerable deviation of the ML model and the climatological SST simulation appears in the North Pacific and is possibly related to missing El Niño variability.

For an overall assessment of the simplified ocean representations we consider the storm track and the cyclone intensity maps. To detect detailed changes of individual cyclone trajectories we use the Lagrangian cluster analysis to group cyclones with particular propagation properties. All results are determined for the winter season (DJF, December to February).

5.1 Validation

The validation of the reference model simulation is divided in two parts: first the mean state using both the filtered variance (storm track) and the counting method (cyclone intensity). Secondly, the interannual variability of the cyclone intensity in relation to teleconnection indices (NAO and ENSO) is considered.

The storm track of the reference simulation with ECHAM/HOPE is shown in Fig. 2a. This agrees with observations (not shown), and reveals, in particular, the known more intense North Atlantic storm track and the more elongated North Pacific storm track; both are simulated with realistic intensities (Stendel and Roeckner 1998).

The simulated cyclone intensity is compared with NCEP re-analysis data mapped to horizontal T42 resolution to reduce the resolution discrepancy with the simulations (Fig. 3a, b). The analysis of the cyclone tracks is restricted to the two Northern Hemispheric ocean basins, the North Pacific in 0°–87°N and 120°E–110°W, and the North Atlantic in 0°–87°N and 100°W–40°E. The cyclone tracks are determined independently and cyclones crossing North America are not considered. Major differences are found in the Mediterranean Sea, southeast and west of Greenland, and in the vicinity of the Aleutian Islands. Instead of the observed maximum southeast of Greenland, a more elongated region extending to Spitsbergen is simulated.

There are several possible reasons for these deviations. A first reason for the overall underestimation of cyclone intensity is the inability to resolve small scale cyclones (note that the resolution of the NCEP data (T42) is still higher than that of the simulation (T30)). Furthermore, the orographic effect of Greenland is not fully captured since the altitude in the model is much lower than observed leading to a reduced orographic trough. A third possible reason is the sea-ice distribution in the reference simulation which differs slightly from the observations, so that the zone of baroclinicity, which is a region of cyclogenesis (Serreze 1995), is shifted southeastward. Note that cyclones travel along regions of intensified baroclinicity (Bosart 1981). This effect might be superimposed to the orographic effect explaining the shift of the observed maximum southeast of Greenland to the west in the simulation. However, the large-scale pattern and the intensity in the Northern Hemisphere is well simulated. Note that details of the cyclone distribution near Greenland and the Aleutian Islands are not found by the storm track analysis (Fig. 2a), hence, the cyclone intensity reveals a more sensitive measure than the bandpass filtered variance. For this reason we use the cyclone intensity in order to analyse the interannual variability of the reference experiment.

In two additional tests we consider the interannual coherency of the Northern Hemispheric cyclone intensity with two major large-scale teleconnection patterns, the NAO and the Niño3 time series indicating the

Fig. 2 Storm track (standard deviation of the 500 hPa geopotential height field, in DJF) of **a** the coupled HOPE reference experiment, and the differences with respect to this reference **b** for varying SST, **c** coupled mixed layer and **d** the climatological experiment. The contours are 5 gpm and above 40 gpm in **a** and 1 gpm in all other panels
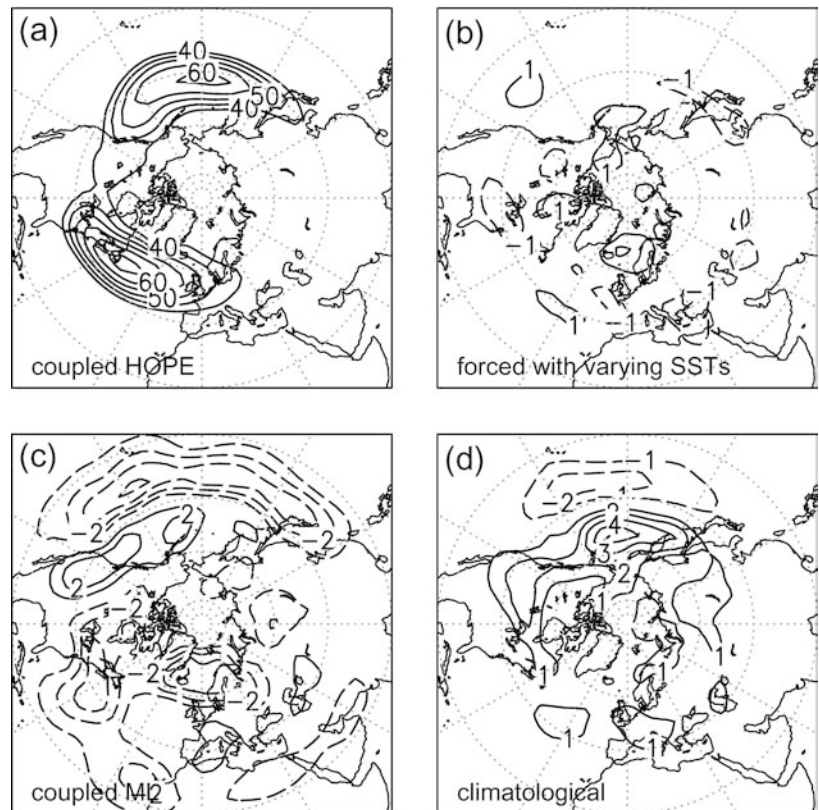
tropical SST west of South America. Composites of the cyclone intensity for positive minus negative NAO states are shown in Fig. 4a (NAO index above or below one standard deviation). The cyclones reveal the known northward shift in the North Atlantic with the NAO (Sickmöller et al. 2000). The equivalence is almost complete in the North Atlantic and the surrounding continents. The simplified experiments show a similar behaviour.

Composites for positive minus negative Niño3 deviations (i.e. El Niño vs. La Niña events) in Fig. 4b show a northeastward shift in the North Pacific. This resembles observational findings by Hoerling et al. (1997) and Sickmöller et al. (2000). The simplified experiment forced with varying SSTs produces a similar shift; the two other simplified simulations do not contain any ENSO-like variability. Note that this absence of ENSO-like variability will play an important role in the interpretation of the differences in the mean state of the simplified experiments later.

The range of the number of cyclones per winter is similar in all experiments varying from 25 to 45 cyclones per winter in the Pacific and from 25 to 50 cyclones per winter in the Atlantic, but the standard deviation is slightly reduced in the Pacific for the simplified experiment. This difference between Atlantic and Pacific agrees with observational findings of Sickmöller et al. (2000). A significant trend in the time series of number of cyclones per winter is not found in any experiment. Thus, we conclude that the reference simulation is able

to realistically reproduce the interannual variability, especially the variations associated with the two major teleconnection patterns.

5.2 Storm tracks

The storm tracks in the three simplified ocean representations are compared to the reference in Fig. 2. The first, remarkable result is that the experiment with the stored, varying SST and sea-ice reproduces the reference experiment with high accuracy (Fig. 2b). This justifies the traditional view that the atmosphere reacts to a passive ocean on short time scales (Bjerknes 1962).

The ML-model (Fig. 2c) alters the variability clearly with distinct changes in the whole Northern Hemisphere. Note, however, that the absolute changes are rather small compared to the interannual variability of the storm track; significance of the changes appears roughly at the 95% level. The deviations have two sources, the absence of ENSO variability, and deviations from the climate mean in the SST and sea-ice (although the model is adjusted to the time mean of the reference simulation). In the North Atlantic, the SST is too warm near Newfoundland and around Iceland, and too cold in the Labrador Sea and west of Spain. Thus, the meridional temperature gradient and hence the synoptic activity are decreased. In the North Pacific between 30°N and 45°N, the SST is slightly too warm, but too cold near Japan, which leads to a northeastward
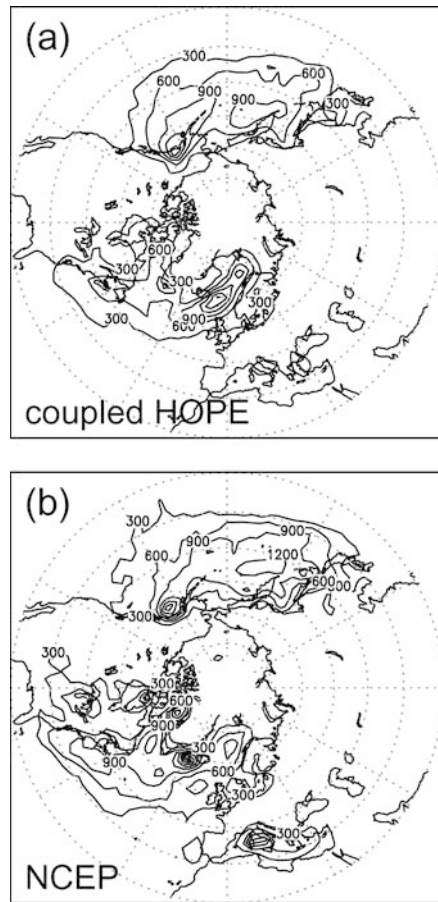
Fig. 3 The cyclone intensity for **a** the coupled HOPE reference experiment (averaged over 100 winter seasons, DJF), and **b** for the NCEP Reanalysis (averaged over 41 winter seasons, DJF). The contours are 300 gpm/1000^3 km^3

displacement of the storm track. The impact of missing ENSO variability is more difficult to detect here, but a possible influence could originate in a nonlinear response.

The climatological experiment (Fig. 2d) shows a northward shift in the North Pacific but no alterations in the North Atlantic. Since the climate mean is perfect (in contrast to the ML experiment), any significant deviation in the North Pacific must originate in the missing ENSO variability. We can deduce that the response has a nonlinear contribution (since otherwise positive and negative ENSO deviations would cancel). This result helps to identify similar causes in the ML experiment (Fig. 2c) with similar, albeit small magnitudes. Obviously, a part of the deviation in the ML experiment is not due to a deviation of the SST from the climate mean. Thus the ENSO impact is superposed to the deviations caused by discrepancies of the mean SST and sea-ice distributions of the ML-experiment.

The result for the storm track already shows that the varying SST and ice is a perfect basis for the atmospheric synoptic variability. The ML result reveals that such simulations have to be analyzed carefully. It is not

assured that the simulated climate mean agrees with the applied forcing. Small deviations may occur, which can hardly be avoided. Surprisingly, it is even better to use the simple climate mean SST and sea-ice in this context.

5.3 Cyclone track intensity

In the experiment forced with varying SST no large-scale differences of the cyclone intensity compared to the coupled HOPE reference experiment appear (Figs. 5a and 3a). This is similar to the storm track comparison (Fig. 2b). There is only a small area at the southern end of the North Pacific storm track region where the intensity is increased.

The ML-experiment shows the largest deviation (Fig. 5b). In the North Atlantic sector an increase of 20% near Great Britain is found whereas near Scandinavia and Newfoundland the cyclone intensity is decreased by 15% to 30%. This leads to a reduction of the area in the ML-experiment where intensified cyclones are identified. To the south of Greenland, an eastward displacement of a large number of cyclones occurs. This is explained by the extended sea-ice cover in the Labrador sea in the ML-model. Note that this shift is not detected by the storm track analysis (Fig. 2c).

In the North Pacific the cyclone intensity of the ML-experiment is shifted northeastward compared to the HOPE experiment with significant differences up to 30%. This can originate in the missing ENSO variability in this experiment superposed with the deviation of the SST and sea-ice (see Sect. 5.2). The decrease south of the Aleutian Islands and near Kamchatka illustrates a further reduction of the area of intense cyclones. This localized decrease is consistent with the El Niño related variability and not seen in the storm track analysis.

The climatological SST experiment shows an increase of the cyclone intensity in the eastern North Atlantic and a decrease over Newfoundland (Fig. 5c). The behaviour in the North Pacific is mainly given by a northward shift, which coincides with the result for the storm track in Fig. 2d. Differences with respect to the coupled HOPE experiment are significant and reach 30%. However, this shift is not fully consistent with the ENSO signal in Fig. 4b and differs also from the ML result mentioned. Therefore, an unambiguous conclusion from this result cannot be drawn.

To summarize, the largest deviations of the cyclone intensity compared to the coupled HOPE reference experiment appear in the ML- and the climatological SST simulation, in particular in the North Pacific sector. In part, these differences can be explained by the missing ENSO-like variability, but depend also on deviations from the mean SST and sea-ice in the ML-experiment. The changes in the North Atlantic are smaller than those in the North Pacific. Obviously, simplified ocean representations can have considerable impacts on the climatology of the cyclone intensity in both regions, even in the case of the correct time-mean forcing.
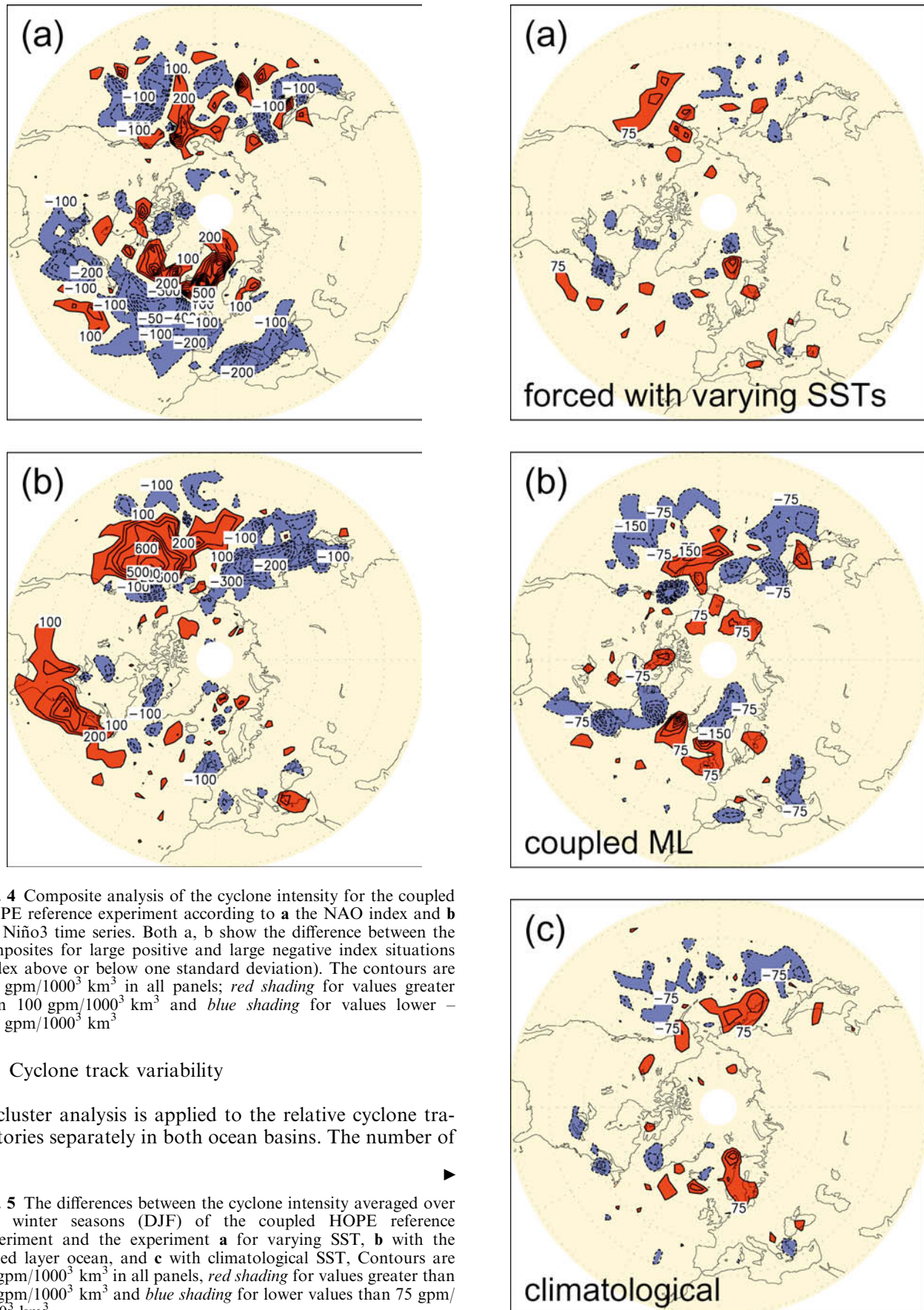
Fig. 4 Composite analysis of the cyclone intensity for the coupled HOPE reference experiment according to **a** the NAO index and **b** the Niño3 time series. Both a, b show the difference between the composites for large positive and large negative index situations (index above or below one standard deviation). The contours are 100 gpm/1000^3 km^3 in all panels; *red shading* for values greater than 100 gpm/1000^3 km^3 and *blue shading* for values lower – 100 gpm/1000^3 km^3

5.4 Cyclone track variability

A cluster analysis is applied to the relative cyclone trajectories separately in both ocean basins. The number of

►

Fig. 5 The differences between the cyclone intensity averaged over 100 winter seasons (DJF) of the coupled HOPE reference experiment and the experiment **a** for varying SST, **b** with the mixed layer ocean, and **c** with climatological SST, Contours are 75 gpm/1000^3 km^3 in all panels, *red shading* for values greater than 75 gpm/1000^3 km^3 and *blue shading* for lower values than 75 gpm/1000^3 km^3

three centroids is chosen since this allows a meteorological interpretation (Blender et al. 1997). In the four experiments there are northeastward (NE), zonally moving (ZO) and stationary (ST) cyclones in the North Atlantic and the North Pacific which coincide with the observed patterns (Sickmöller et al. 2000). The cluster centroids of the experiments are shown in Fig. 6 for both regions. The coordinate dx denotes the relative displacement in zonal direction, dy in meridional direction, and the bars denote the standard deviations in both directions at daily time steps obtained in the coupled HOPE experiment.

The three centroids in the four simulations share properties with the observed centroids: (1) the Pacific NE cyclones move meridionally after two days (in contrast to the Atlantic NE centroid); (2) the Pacific ZO centroid reaches higher latitudes than the Atlantic ZO
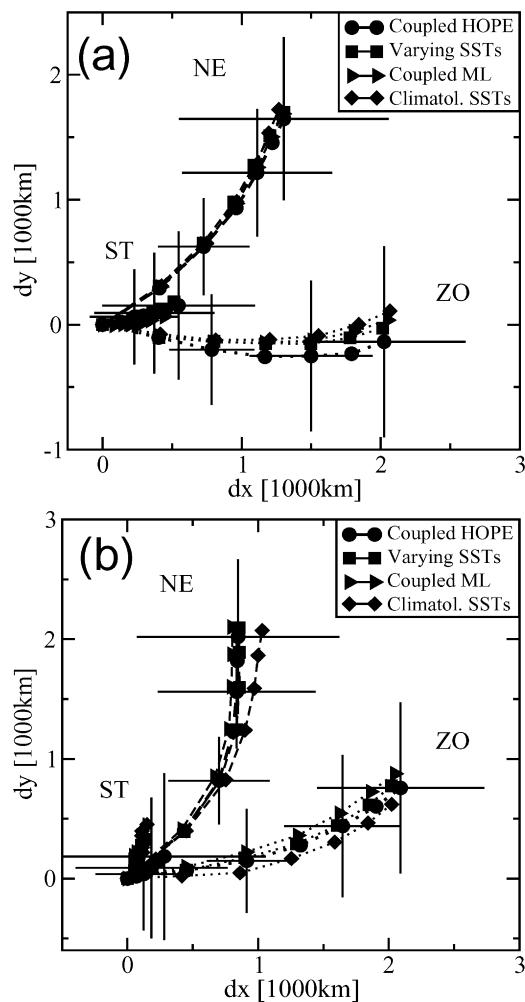
centroid at the end of the lifetime of three days. In total, the North Pacific centroid pattern looks like a counterclockwise rotated version of the centroid pattern in the North Atlantic. This agrees with observations.

The comparison of the coupled HOPE experiment with the simplified experiments shows no significant differences of the cluster centroids. The distribution of the numbers of registered cyclones among the clusters is presented in Table 1 for the four experiments. The total numbers of cyclones agree in all experiments with deviations below 5%; the cluster occupation numbers agree to within 10%. The small differences between the coupled HOPE and the coupled ML- and climatological SST experiments are significant at a level of 99% in both basins.

The cyclones within a particular cluster can be used to determine a cyclone intensity map which indicates the region preferred by the cyclones within the corresponding cluster. Figure 7 shows the intensity maps for both ocean basins and the three clusters obtained in the HOPE simulation. Some differences of the cyclone cluster intensities between the experiments are mentioned later (not shown): The increase of intense cyclones near Great Britain (coupled ML-experiment) and in Scandinavia (climatological experiment) shown in Fig. 5b, c are mainly caused by an increase of zonally moving cyclones. The northward displacement in the North Pacific in these two experiments is due to northward displacement of NE and ZO cyclones. In observations, Sickmöller et al. (2000) find a correlation between the Southern Oscillation index and NE and ZO cyclones, but not with ST cyclones. This is an additional support for connection between the displacement of the cyclones and ENSO. Note that since we use the cyclone intensity (number weighted by the geopotential height

Fig. 6 Cluster centroids of the relative cyclone trajectories in **a** the North Atlantic and **b** the North Pacific obtained in the four experiments (as indicated in the legend). The centroids are northeastward oriented (*dashed*), zonal (*dotted*) and stationary cyclones (*solid*). The *horizontal* and *vertical bars* denote the standard deviation of the centroids of the coupled HOPE reference experiment at daily time intervals. dx is the relative displacement in zonal direction and dy in meridional direction

Table 1 Number of cyclones with an age of at least three days for all clusters (northeastward: NE, zonal: ZO, stationary: ST, and total: TO) and all experiments in the two regions North Atlantic (NA) and North Pacific (NP) in 100 winter seasons (99 winter for varying SST)

Experiment	Cluster	Number of cyclones			
		NA	(%)	NP	(%)
Coupled HOPE	NE	1751	(44.1%)	1431	(40.4%)
	ZO	1040	(26.2%)	1257	(35.5%)
	ST	1181	(29.7%)	857	(24.1%)
	TO	3972		3545	
Coupled ML	NE	1664	(42.8%)	1244	(37.1%)
	ZO	1093	(28.1%)	1275	(38.0%)
	ST	1134	(29.1%)	834	(24.9%)
	TO	3891		3353	
Varying SST	NE	1637	(41.9%)	1392	(39.2%)
	ZO	1103	(28.2%)	1277	(36.0%)
	ST	1170	(29.9%)	880	(24.8%)
	TO	3910		3549	
Climatolog. SST	NE	1635	(42.4%)	1428	(41.0%)
	ZO	1128	(29.1%)	1260	(36.2%)
	ST	1115	(28.7%)	796	(22.8%)
	TO	3878		3484	

Fig. 7 Cyclone intensity of the coupled HOPE experiment in **a**, **c**, **e**, the North Atlantic and **b**, **d**, **f** the North Pacific decomposed in the three clusters, northeastward (*NE*; **a, b**), zonally moving (*ZE*; **c, d**), and stationary cyclones (*ST*; **e, f**). The *contour interval* is 100 gpm/1000³ km³ in *all panels* except for **f** with 50 gpm/ 1000³ km³
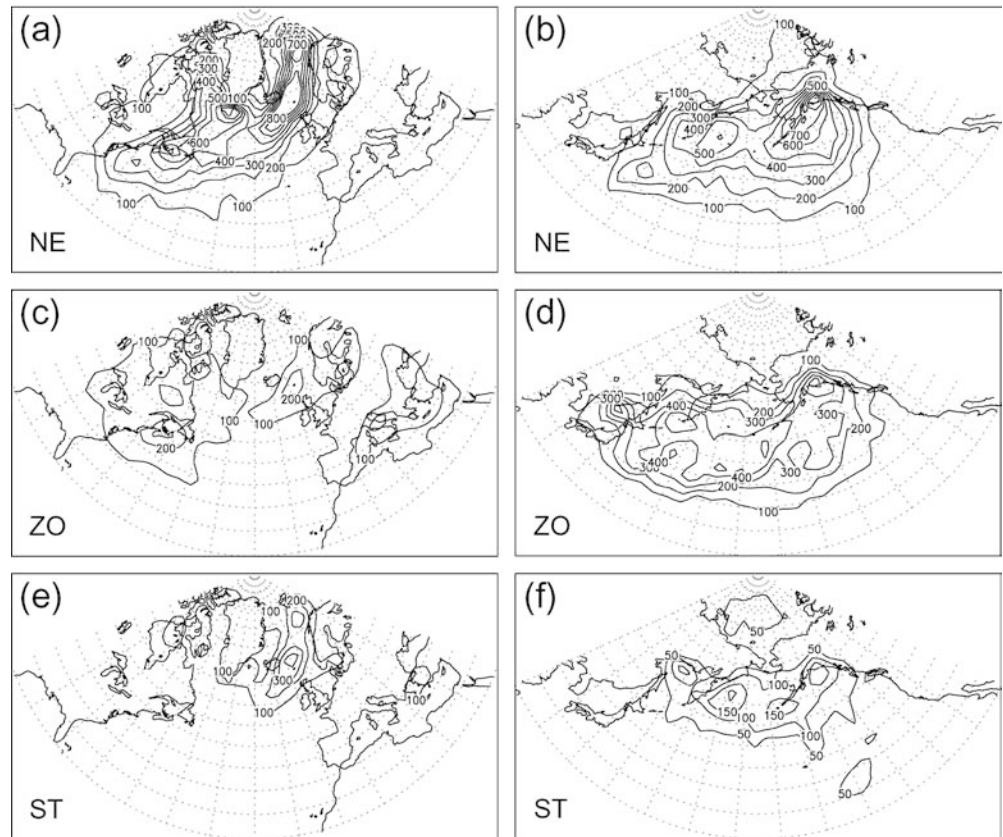
gradient) these patterns deviate from the observed patterns of the number density within the clusters.

In summary, the cluster analysis of individual cyclone tracks shows that the spatial structure of the three different types of cyclone tracks (the cluster centroids) are similar in all experiments and agree with the observations. Moreover, the total numbers of cyclones and the numbers within the clusters differ only slightly between the four experiments.

6 Summary and discussion

This study evaluates the impact of a ML-model and simple ocean boundary conditions on synoptic cyclones in the Northern Hemisphere. The cyclones are simulated with the atmospheric model ECHAM which is run with a resolution of T30 (3.75° × 3.75°). A coupled simulation using ECHAM and the ocean general circulation model HOPE is used as a reference. Simpler experiments are performed with ECHAM and a variable depth mixed-layer model, an independent varying ocean boundary and a climate (annual mean) ocean boundary, both are obtained from the coupled ECHAM/HOPE simulation. The experiments are consistent with respect to the climate mean of the SST and the sea-ice boundary (in addition to the ML-simulation, which is adjusted to the climate mean).

The cyclones are tracked automatically with the identical scheme. Intensity maps are determined by a weighting of their number density with the mean geopotential height gradient. The comparison of the reference experiment with observations shows sufficient agreement. Displacements of the cyclone intensity, mainly in the North Atlantic, can be explained by the coarse resolution of the atmospheric model. Note that these changes are not found in the band-pass filtered variance suggesting that it is a more valuable diagnostic measure of model sensitivity and climate change.

The experiment forced with varying SST obtained from the coupled HOPE reference experiment yields no deviations of the cyclone intensity patterns compared to the reference experiment. However, in the coupled mixed layer and the climatological experiment, there is a distinct northward shift of the storm tracks and cyclone intensities in the North Pacific. As there are no differences in the trend behaviour between all experiments a possible reason for this shift in the Pacific is the missing ENSO variability. Moreover, the difference pattern in the North Pacific and the ENSO variability pattern of the reference experiment (illustrated by the composite analysis) show similarities, substantiating the idea that the coarse resolution model experiments without ENSO-like variability terminate in shifted mean cyclone positions in the Pacific. Note that this also implies that there is a nonlinear response of long-term cyclone intensity to

ENSO-like variability. In the ML-experiment simulated deviations of the mean SST and sea-ice from the climate mean are a further source of deviations. These are also responsible for the decrease of cyclones in the North Atlantic.

The variability of the individual tracks is analyzed by a cluster analysis of the relative trajectories. These are grouped into three centroids: north-eastward, zonally moving, and approximately stationary cyclones. The centroids are almost identical in all four experiments and in the observations. Thus, the structure of the trajectories is not affected by the ocean variability. Therefore, we conclude that the splitting in three clusters and the relative trajectories can be traced back to the internal, nonlinear atmospheric dynamics in constant land-sea contrast and orography. Displacements of the cyclone intensity are due to a shift of the cyclone track with no change of the internal variability.

References

Bjerknes J (1962) Synoptic survey of the interaction between sea and atmosphere in the North Atlantic. Geophys Publ 24: 116–145

Blackmon ML (1976) A climatological spectral study of the 500 mb geopotential height of the Northern Hemisphere. J Atmos Sci 33: 1607–1623

Blender R, Fraedrich K, Lunkeit F (1997) Identification of cyclone-track regimes in the North Atlantic. Q J R Meteorol Soc 123: 727–741

Blender R, Schubert M (2000) Cyclone tracking in different spatial and temporal resolutions. Mon Weather Rev 128: 377–384

Bosart LF (1981) The President's Day snowstorm of 18–19 February 1979: a subsynoptic-scale event. Mon Weather Rev 109: 1542–1566

Dommenget D (2000) Large-scale SST variability in the midlatitudes and in the tropical Atlantic. PhD Thesis, pp 118

Haak U, Ulbrich U (1996) Verification of an objective cyclone climatology for the North Atlantic. Meteorol Z 5: 24–30

Hartigan JA, Wong MA (1979) A k-means clustering algorithm. Appl Stats 28: 100–108

Hodges KI (1994) A general method for tracking analysis and its application to meteorological data. Mon Weather Rev 122: 2573–2586

Hoerling MP, Kumar A, Zhong M (1997) El Niño, La Niña, and the nonlinearity of their teleconnections. J Clim 10: 1769–1786

Karaca M, Müller D (1991) Mixed-layer dynamics and buoyancy transports. Tellus 43: 350–365

König W, Sausen R, Sielmann F (1993) Objective identification of cyclones in GCM simulations. J Clim 6: 2217–2231

Lambert SJ, Sheng J, Boyle J (2002) Winter cyclone frequencies in thirteen models participating in the Atmospheric Model Intercomparison Project (AMIP1). Clim Dym 19: 1–16

Lau N-C (1988) Variability of the observed midlatitude storm tracks in relation to low-frequency changes in the circulation pattern. J Atmos Sci 45: 2718–2743

Legutke S, Voss R (1999) The Hamburg atmosphere–ocean coupled circulation model ECHO-G. Tech Rep 18, Deutsches Klimarechenzentrum, Hamburg, Germany, pp 62

Murray RJ, Simmonds I (1991) A numerical scheme for tracking cyclone centres from digital data, Part I: development and operation of the scheme. Aust Meteorol Mag 39: 155–166

Raible CC, Luksch U, Fraedrich K, Voss R (2001) North Atlantic decadal regimes in a coupled GCM simulation. Clim Dyn 17: 321–330

Roebber PJ, Tsonis AA, Elsner JB (1997) Do climate simulations from sea surface temperature forced models represent actual dynamics? Nonlinear Proc Geophys 4: 93–100

Roeckner E, Arpe K, Bengtsson L, Christoph M, Claussen M, Dümenil L, Esch M, Gioretta M, Schlese U, Schluzweida U (1996) The atmospheric general circulation model ECAHM-4: Model description and simulation of present-day climate. Tech Rep 218, Max-Planck-Institut für Meteorologie, Hamburg, Germany, pp 90

Schubert M, Perlwitz J, Blender R, Fraedrich K, Lunkeit F (1998) North Atlantic cyclones in CO_2-induced warm climate simulations: Frequency, intensity, and tracks. Clim Dyn 14: 827–838

Serreze MC (1995) Climatological aspects of cyclone development and decay in the Artic. Atmosphere-Ocean 33: 1–23

Sickmöller M, Blender R, Fraedrich K (2000) Observed winter cyclone tracks in the northern hemisphere in re-analysed ECMWF data. Q J R Meteorol Soc 126: 591–620

Sinclair MR (1994) An objective cyclone climatology for the southern hemisphere. Mon Weather Rev 122: 2239–2256

Sinclair MR (1997) Objective identification of cyclones and their circulation intensity, and climatology. Weather Forecast 12: 595–612

Stendel M, Roeckner E (1998) Impacts of the horizontal resolution on simulated climate statistics in ECHAM-4. Tech Rep 253, Max-Planck-Institut für Meteorologie, Hamburg, Germany, pp 57

Terray L, Valcke S, Piacentini A (1998) The OASIS coupler user guide, version 2.2. Tech Rep TR/CMGC/98-05, CERFACS, pp 77

Ueno K (1993) Interannual variability of surface cyclone tracks, atmospheric circulation patterns, and precipitation patterns in winter. J Meteorol Soc Japan 71: 655–671

Wallace JM, Lim G-H, Blackmon M-L (1988) Relationship between cyclone tracks, anticyclone tracks and baroclinic wave-guides. J Atmos Sci 45: 439–462

Wolff JO, Maier-Reimer E, Legutke S (1997) The Hamburg ocean primitive equation model HOPE. Techn Rep 13, Deutsches Klimarechenzentrum, Hamburg, Germany, pp 98